Testing the Two-State Model: Anomalous Effector Binding to Human Hemoglobin†

Michael C. Marden,* E. Starr Hazard, and Quentin H. Gibson

The Section of Biochemistry and Molecular Biology, Cornell University, Ithaca, New York 14853

Received May 28, 1986; Revised Manuscript Received August 1, 1986

ABSTRACT: Three allosteric states are required to describe the relaxation of (carbon monoxy)hemoglobin following flash photolysis. Combined absorbance and fluorescence probes were used. The absorbance signals consist of a component corresponding to ligand recombination and a component for the R–T transition. The fluorescence of 8-hydroxy-1,3,6-pyrenetrisulfonate (HPT), an analogue of 2,3-diphosphoglycerate, shows rates and amplitudes correlated with the absorbance transients. Measurements were made at pH 6, 6.5, and 7.0 at CO partial pressures of 0.1 and 1 atm. The fractional photolysis was varied in each case to change the initial distribution of the R states. Data show an immediate absorbance change due to ligand dissociation, while the changes in the ligand isosbestic and the fluorescence signals occur with time constants of 80 μs (at pH 6.5). The signals then show a biphasic return to equilibrium, characteristic of the allosteric system. The measurements provide three independent probes of the kinetics of the substates of hemoglobin. Although the ligand binding data can be generally represented by a two-state model, the fluorescence data require T states with different affinities for HPT.

The static and kinetic ligand binding properties of hemoglobin (Hb) have been extensively studied (Antonini & Brunori, 1971; Shulman et al., 1975; Gibson, 1978). It has been appreciated for 75 years that cooperative interactions within this tetrameric heme protein make the ligand binding properties more complex than a linear sum of independent subunits. Kinetic studies showing two phases in the bimolecular recombination of oxygen or carbon monoxide (CO) led to a distinction of the fast reacting R form and the slower T form (Gibson, 1959). This implies at least 10 states for the tetramer, having 0–4 ligands in two possible forms. The detailed interconnection of these 10 states remains unknown, despite the vast amount of data collected.

The first ordered scheme for the tetramer was the two-state (MWC) model of Monod, Wyman, and Changeux (Monod et al., 1965). This model assumes all R states have the same ligand binding rates and all the T states are similarly degenerate. The free energy spacing between R states is greater than that of the T states, allowing a conversion from the deoxy T state to the R state when completely ligated. This two-state model, with respect to ligand binding, provides a general description of both flash photolysis and stopped-flow kinetics, as well as the sigmoidal equilibrium curves.

Recent interest in Hb cooperativity and the validity of the two-state model has led to a better definition of which tetramer properties may be described by only two states (Smith & Ackers, 1985; Johnson, 1986; Edelstein & Edsall, 1986). This work arose in part from claims that the two-state model is inconsistent with the experimental values for the dimer–tetramer equilibrium (Weber, 1984). Weber's claim is valid in a strict two-state model, but not when the dimer–tetramer equilibrium of the T states is allowed to vary with the number of ligands bound (Edelstein & Edsall, 1986).

The two-state model usually requires expansion to account for ligand binding differences in the α and β chains within the tetramer (Saffran & Gibson, 1978). This leads to a model that can simulate a large variety of data. Although a great simplification and a useful tool, the expanded two-state model has many degrees of freedom and is difficult to test thoroughly with only ligand binding results.

Equilibrium studies using NMR techniques show that two allosteric states are insufficient to describe the Hb tetramer (Viggiano & Ho, 1979; Miura & Ho, 1984). Kinetic studies using hybrid tetramers also indicate that the two-state model does not provide a complete description of Hb (Blough & Hoffman, 1984; Blough et al., 1984; Simolo et al., 1985). The next level of refinement is therefore in understanding the deviations from a two-state behavior, which will require a combination of probes of the allosteric and ligation states.

Three probes of the tetramer states were used in this study to test more completely the predictions of the two-state model. In addition to the ligand binding signal, the R–T transition was observed at a wavelength isosbestic for the ligand photolysis (Sawicki & Gibson, 1976). This isosbestic measurement provides a direct observation of the heme groups converting between R and T states.

The third probe is the fluorescence of the dye molecule 8-hydroxy-1,3,6-pyrenetrisulfonate (HPT), which binds more strongly to the T state with a stoichiometry of 1; HPT is displaced by inositol hexakis(phosphate) (IHP) and 2,3-diphosphoglycerate (DPG) (MacQuarrie & Gibson, 1972). Serving as a fluorescent analogue of DPG, HPT lowers the oxygen affinity of Hb by a factor of 2, while DPG lowers the affinity 5-fold and IHP by a factor of the order of 100. After ligand photodissociation from the R state, dye binds to the newly formed T state molecules and the fluorescence intensity decreases due to quenching by the heme. The fluorescence signal then shows a biphasic return to the initial state.

The reactions were studied as a function of pH, which shifts the R–T equilibria, and over a range of fractional photolysis that changes the initial distribution of the R states. Two CO concentrations were used to provide information on the competition between the R–T transition and ligand recombination to the fast R form.

† This work was supported in part by the National Institutes of Health (Grant GM-14276) and the National Science Foundation (Grant 79-10446).

0006-2960/86/0425-7591$01.50/0

The data presented here require the HPT binding properties of the tetramer to be dependent on the degree of ligation. The biphasic fluorescence signal shows more fast phase than is allowed within a two-state framework which requires all T states to have the same dye affinity.

Experimental Procedures

Human red blood cells, obtained from Tompkins Community Hospital, were washed in 0.15 M NaCl, centrifuged, and frozen as droplets in liquid nitrogen. The red cell pellets were thawed in 3 volumes of 1 mM tris(hydroxymethyl)aminomethane hydrochloride (Tris-HCl), pH 8.5; the hemolystate was brought to 0.1 M NaCl with solid NaCl. The crude stock was centrifuged at 8000*g* for 10 min, and the supernatant was layered onto a 2.5 × 30 cm Sephadex G-25 (medium) column equilibrated with 50 mM Tris, pH 8.5, and 0.1 M NaCl and eluted at 1 mL/min. The stock was dialyzed overnight against 1 mM Tris-HCl, pH 8.5, and passed through a final desalting column of 2 cm of Sephadex G-25 (Pharmacia), 2 cm of AG50WX8 cation-exchange resin, ammonium form (Bio-Rad), 2 cm of Dowex-1 acetate form, and 20 cm of mixed-bed resin AG501-X8(D) (Bio-Rad). The stock was concentrated on Centriflo ultrafiltration cones, equilibrated with 1 atm of CO, and refrozen in liquid nitrogen.

The fluorescent dye 8-hydroxy-1,3,6-pyrenetrisulfonic acid trisodium salt (HPT) (Kodak laser grade) was the same dye previously used (MacQuarrie & Gibson, 1972). The low-pH form absorbs at 370 and 404 nm; these bands are replaced at high pH by a band at 457 nm. Samples were in tonometers attached to cuvettes of 2-mm optical path length. Standard samples were 50 mM [bis(2-hydroxyethyl)amino]tris(hydroxymethyl)methane hydrochloride (Bis-Tris-HCl), 10 μM Hb tetramer, and 10 μM dye. The fluorescence intensity was linear with dye concentration in this region.

Since inositol hexakis(phosphate) (IHP) displaces HPT, the amount of fluorescence change due to the change in sample absorbance could be measured. Flash photolysis in the presence of IHP and HPT showed the full absorbance changes for ligand binding and a 2.5% change in fluorescence. Since HPT does not bind under these conditions, the result must be due to the difference in the Hb filter effect between the deoxy and ligand-bound states. Since the total change in fluorescence varied from 20% at pH 6 to 30% at pH 7, the correction for the filter effect, although small, is not negligible.

Flash photolysis measurements were performed by using a Phase-R dye laser delivering 250 mJ in 500-ns pulses at 575 nm. One hundred percent photolysis is not possible due to geminate ligand recombination (Duddell et al., 1980); with the pulse length used, a maximum photolysis of 92% was obtained. For observation, a Xenon arc lamp was filtered (Corning 5-57) for excitation of the dye between 370 and 480 nm and also to provide for absorption studies at 436 and 426 nm. The transmitted light passed a Spex monochromator of 3-nm bandwidth, and the photomultiplier signal was recorded on a Biomation Model 805 transient digitizer interfaced (Metrabyte PIO12) to an IBM PC.

The fluorescence emission, with maximum at 510 nm, was detected at right angles to the excitation beam by using a light guide, filters, and photomultiplier and recorded on a transient digitizer. Yellow glass (Corning 3-70) was used to limit the scattered excitation light to less than 2% of the emission intensity. The scattered laser pulse could not be excluded completely, although a polarizer and didymium glass (Corning 1-60) helped. To avoid a long recovery time, the photomultiplier was gated, using a monostable version of a standard gating circuit (Hamilton, 1971). The signal was reduced by a factor of 30 during the gate (typically 10–20 μs) resulting in an overload spike of a few microseconds for the scattered photolysis pulse.

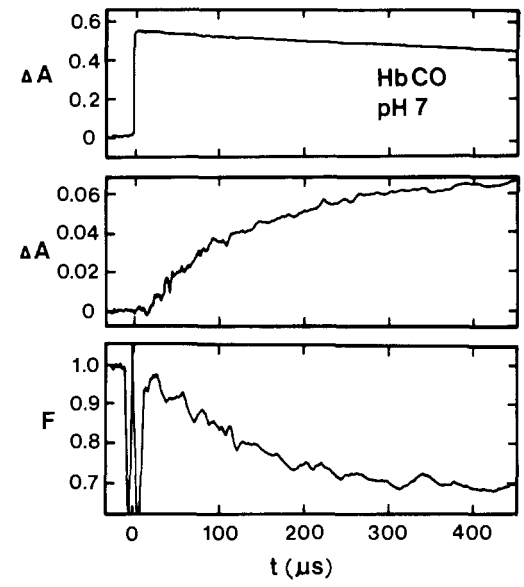

FIGURE 1: Data for human Hb at pH 7 and 0.1 atm of CO. The three signals are the ligand binding absorbance change detected at 436 nm (top), the R–T transition detected at 425.8 nm (middle), and the change in HPT fluorescence (bottom). The photomultiplier was gated for the ΔF data and shows only the laser pulse during the first 20 μs.

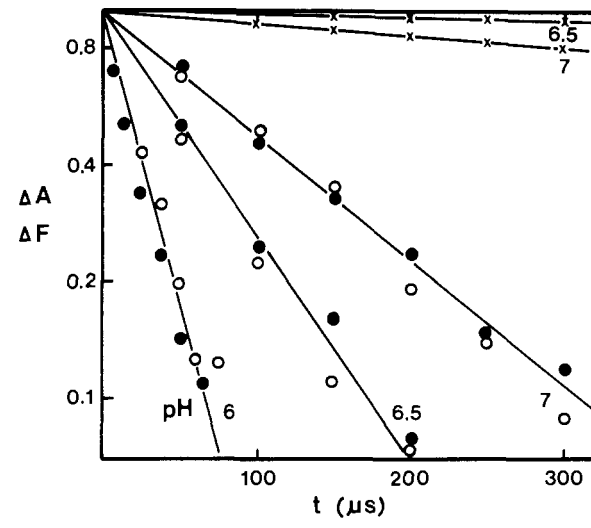

FIGURE 2: The normalized R–T transition kinetics at pH 6, 6.5, and 7, as observed by the absorbance change at 425.8 nm (●) and the decrease in HPT fluorescence (○). Also shown are the ligand binding kinetics observed at 436 nm (×).

Results

Kinetic traces for the three types of signal are shown in Figure 1. The top portion shows the CO rebinding curve; photodissociation occurs immediately with the laser pulse, and there is little recombination on the time scale of the figure. At an isosbestic point (425.8 nm) for the ligand reaction, the R–T transition can be observed (middle section of Figure 1). A decrease in fluorescence intensity is observed as the HPT binds to the T-state tetramer (bottom section of Figure 1).

The rate of the R to T transition decreases as the pH is raised, as shown in Figure 2. The fluorescence and ligand isosbestic signals had the same rate for all sample conditions. Also shown in Figure 2 are the corresponding absorbance

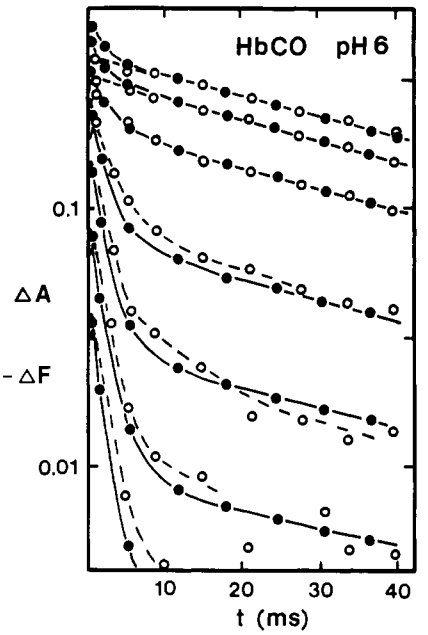

FIGURE 3: Flash photolysis kinetics of Hb at pH 6 and 0.1 atm of CO, showing ΔA at 436 nm (●) and the increase in fluorescence (○). The initial decrease in fluorescence (Figures 1 and 2) is too rapid to be seen on this plot. The fractions photolyzed were $z = 0.92$, 0.88, 0.66, 0.45, 0.25, 0.15, and 0.07. The ΔF data were scaled to match the ΔA data at maximum signal.

signals at 436 nm for the ligand recombination. The R–T transition is slow enough at pH 7 to allow some R-state recombination at 0.1 atm of CO.

Ligand recombination, observed at 436 nm, and fluorescence results at various levels of ligand photolysis (z) at pH 6 are shown in Figure 3. The absorbance and fluorescence data were superimposed by matching the maximum signals for the slow phase. Note that the initial decrease in fluorescence (Figures 1 and 2) occurs in the first 0.1 ms and is not evident in Figure 3. At full photolysis and low [CO], the transition from R to T is nearly complete and the kinetics show mainly a slow phase. The small fast phase in ΔA is due to dimers that have R-state binding rates; a fast component at full photolysis is absent from the fluorescence signal.

At intermediate levels of photolysis, there is initially a distribution of R states, which come to equilibrium with the T states. This R-T mixture produces the biphasic kinetics as observed in both the absorption and fluorescence signals. There is an excellent correlation in the rate and amplitude of the slow phase for the two signals. The amount of fast fluorescence is dependent on pH and [HPT].

Results at pH 6 showed the largest amplitude of fast phase in the fluorescence signal. At low fractional photolysis, the fast component accounts for nearly all of the signal. It may even be a substantial fraction of the total ΔF observed at maximum photolysis ($z \rightarrow 1$). At pH 6 with 50% photolysis ($z = 0.5$), the fast component exceeds 40% of the total signal at maximum photolysis. The amplitude of the fast phase, normalized with respect to the total signal at maximum photolysis ΔF_{MAX}, is shown vs. the fractional photolysis (z) in Figure 4 for pH 6, 6.5, and 7. The curves were measured at three dye concentrations at pH 6 (Figure 5), [HPT]/[Hb] = $^1/_4$, 1, and 8. The ratio of the fast ΔF to ΔF_{MAX} decreased at higher [HPT].

Also shown for comparison in Figures 4 and 5 is the fraction of tetramer in the R_2 state (two ligands bound) just after the flash. This fraction was calculated for different ratios of the quantum yields for the two chains, since the yields of the α and β chains are not necessarily the same. Separate photodissociation experiments indicate a ratio of not more than 2 for the yields (data not shown). The yields and observations discussed here refer to the bimolecular phase; the geminate phase is not included.

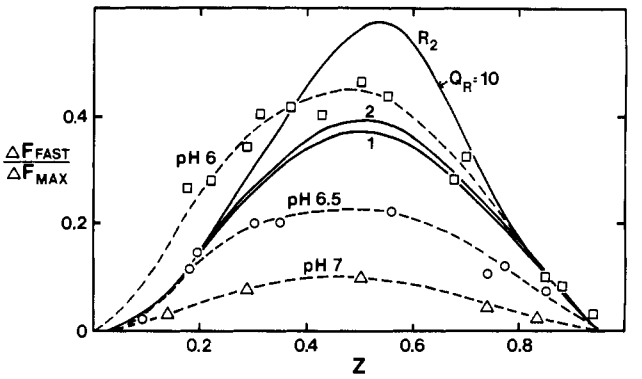

FIGURE 4: The fast component of the fluorescence signal, normalized to the maximum ΔF ($z \rightarrow 1$), vs. fractional photolysis (z). The data shown are for [HPT] = [Hb] = 10 μM with 0.1 atm of CO at pH 6 (□), 6.5 (○), and 7 (△). The solid lines are the fraction of R_2 just after the flash, calculated for subunits with a ratio of quantum yields Q_R = 1, 2, and 10.

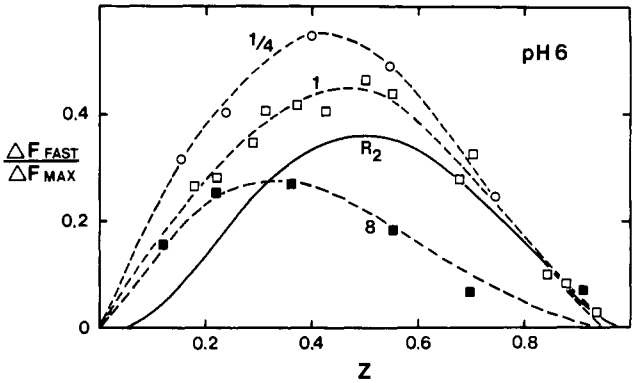

FIGURE 5: The normalized fast component of ΔF vs. z, as in Figure 4. Data are for 10 μM Hb tetramer with [HPT]/[Hb] = $^1/_4$ (○), 1 (□), and 8 (■). Enhancement of fast ΔF at low [HPT] indicates T_2 binds HPT with higher affinity than T_0.

The association or dissociation rate of HPT binding might limit the rates of the observed fluorescence signals. The HPT binding time constants are short compared to stopped-flow mixing times of 1.5 ms (MacQuarrie & Gibson, 1972). Results here extend the maximum association time constant to 25 μs, observed at pH 6. A half-time of 50 μs was observed at pH 6.5 and was independent of HPT concentration. The shortest dissociation half-time observed was 100 μs for samples equilibrated with 1 atm of CO. The good correlation of fluorescence and absorption rates indicates that the binding rates of HPT are not a limiting factor.

Since addition of IHP causes a large shift toward the T state, the effect of the fluorescent probe HPT was studied. Samples of stripped Hb with and without 10 μM HPT showed no change in the ligand binding kinetics. However, only 25% of the T-state tetramers have dye bound in the usual experimental conditions. An effect was seen at 80 μM HPT at pH 6; at low photolysis levels, the fraction of ligand binding in the slow phase increased by a factor of 1.5, while IHP caused an increase of over a factor of 10.

Note that the correlation of amplitudes of ΔA and ΔF in Figure 3 is a special case. The amount of fast ΔF decreases at higher pH (Figure 4), while the amount of fast ΔA increases.

Discussion

Ligand and dye binding kinetics of Hb after flash photolysis involve multiple processes whose amplitudes are dependent on the initial distribution of the R states and their equilibria with the T states. Multiple probes are necessary in determining the many equilibria involved in the tetramer. The data presented here provide three independent indicators of the state of Hb during the R–T transition and subsequent ligand recombination.

The absorbance difference at 436 nm monitors the ligand binding reaction. The dependence of this signal on fractional photolysis reflects the allosteric behavior of Hb. The R to T rate can be inferred from the competition between R-state ligand binding and the R to T transition. From results vs. fractional dissociation the individual equilibria can be estimated, given in the two-state model as

$$T_0/R_0 = L \qquad T_i/R_i = Lc^i \tag{1}$$

with i the number of ligands bound. For the data shown here, $1/c \cong 500$, and L, which is pH-dependent, is on the order of 10^6–10^7.

The signal at 425.8 nm monitors heme absorbance changes without contribution from ligand dissociation from the R state. The isosbestic wavelength is found by nulling ΔA at short times at full photolysis; this requires $\Delta A = 0$ for the states R_4 and R_0. This R_4–R_0 isosbestic signal provides a direct measure of the R to T rate, which was found to be independent of fractional photolysis. This indicates that the R to T rates are independent of ligation state and the shift in equilibria must be due to changes in the reverse rates. Previous measurements indicate that at pH 9 the R to T rate decreases at lower z (Sawicki & Gibson, 1976).

Since only one dye molecule binds per Hb tetramer, the fluorescence signal detects changes in the tetramer state, rather than in the heme state as in the absorbance changes. After the flash, R tetramer converts to the T state, which takes up dye, resulting in a quenching of the fluorescence. Because the ratio of T_0 to R_0 is large ($L \cong 10^6$), dye originally bound to T_0 will be released at the slow T-state ligand binding rate. However, for an R–T pair populated in roughly equal amounts at equilibrium, ligand binding to the fast R form will be followed by a readjustment of the R–T concentrations, which depopulates the T state, resulting in a fast fluorescence signal.

With values of $1/c$ on the order of 500, it is clear that only one R_i–T_i pair can be present in roughly equal populations. The key pair for the data presented here is R_2–T_2, since the equilibrium ratio T_2/R_2 shifts from 0.6 at pH 7 to about 10 at pH 6, as determined from simulations of the ligand binding data. Thus the doubly liganded states play the crucial role in the amount of fast ΔF. As shown in Figure 4, the amount of fast ΔF has the general form of R_2 (formed by the laser pulse) vs. fractional photolysis and is pH-dependent.

A striking anomaly is the amount of fast ΔF at pH 6, which actually exceeds the fraction of R_2 formed by the laser pulse. A difference in quantum yields for the two types of subunit offers one possible explanation. In the limit of a large ratio of yields, one type of subunit will be photodissociated before the other, resulting in the production of a nearly pure R_2 tetramer at $z = 0.5$. However, measurements of the yields showed a ratio of no more than 2; therefore, the large amount of fast ΔF at pH 6 cannot be explained by differences in the quantum yields.

Substate Contribution to the Observed Signals. The amplitudes of both the isosbestic absorbance signal and the change in fluorescence depend on the initial distribution of R states and on the R–T equilibria. The amplitudes of these signals provide a second measure of the allosteric equilibria.

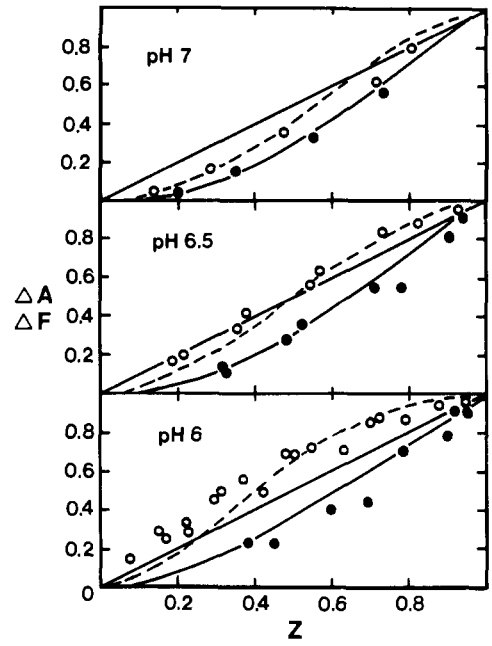

FIGURE 6: Total ΔF (---O---) and ΔA at 425.8 nm (●), isosbestic for ligand recombination, vs. fractional photolysis at pH 6, 6.5, and 7. Lines are simulations using the two-state model, showing the effect of changing the equilibrium ratio T_2/R_2 which varied from 0.6 at pH 7 to 10 at pH 6.

The first step in the analysis is to obtain the initial distribution of R states just after the laser pulse. For a photolysis pulse short compared to microstate interconversion times, this is given by the binomial distribution as a function of fraction of sites photodissociated (z). For unequal quantum yields of the bimolecular phase, the subunits must be treated separately.

Equal Tetramer Weights for ΔF. The second step in the simulation is the calculation of the R–T equilibrium. At low ligand concentrations, this reaction will be complete before appreciable ligand recombination. The amount changing from R to T depends on the amounts of R_i and their equilibria with T_i and will be reflected in the amplitudes of the isosbestic and fluorescence signals. The normalized amplitudes of the two signals are different functions of z. The isosbestic signal falls off more rapidly as z is decreased, as shown in Figure 6. At pH 7 the two signals are nearly the same, while at pH 6 differences exceed a factor of 2.

Simulations of the amplitudes of the fluorescence and isosbestic absorption signals require two different methods of weighting the tetramer states. Since each Hb tetramer binds one dye molecule, the amplitudes of the fluorescence signals (Figure 7, bottom) are calculated with the tetramers given equal weight. The maximum amplitude is calculated by assuming the R–T transition is complete (low [CO]) and is given by the difference in the amount of R state just after photolysis ($t = 0$) and after the R–T transition:

$$\Delta F = \sum_{i=0}^{4} R_i(t = 0)/(1 + 1/Lc^i) \tag{2}$$

where $R_i(t = 0)$ is the initial fraction of tetramers with i ligands bound and the second term accounts for the R–T equilibrium. With all tetramers providing equal signal size, the simulation approaches the curve for $1 - R_4$ in the limit of large L (assuming large R_4/T_4), and the curve R_0 is obtained for the small L limit (assuming $L = T_0/R_0$ is still $\gg 1$).

Tetramer Weights for the Ligand Isosbestic Signal. A different function of z is obtained by assuming the signal is

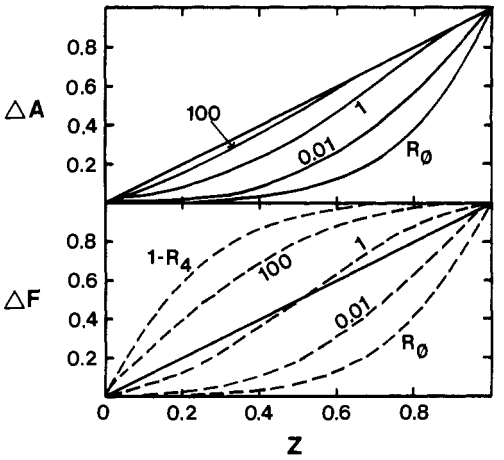

FIGURE 7: Simulations of total ΔF (eq 2) and ligand isosbestic ΔA at 425.8 nm (eq 3) vs. z, as in Figure 6. Values given are the equilibrium ratio T_2/R_2. With tetramers given equal weight as for ΔF (eq 2), the curves show a greater variation, with limiting values equal to the fraction of R_0 for small L and $1 - R_4$ for large L.

proportional to the number of deoxy hemes involved in the R–T transition. The form used for the R_4–R_0 isosbestic ΔA weights the tetramers in proportion to the number of deoxy hemes:

$$\Delta A_{iso} = \sum_{i=0}^{4}(1 - i/4)R_i(t = 0)/(1 + 1/Lc^i) \qquad (3)$$

These simulations (Figure 7, top) show a smaller variation as $T_2/R_2 = Lc^2$ is varied, and at large L (for example, with IHP) the simulated values are equal to the fraction photolyzed (z).

When the equilibrium ratio T_2/R_2 is small, the two types of weighting show nearly the same curve since the main contribution is from $R_0 \rightarrow T_0$ and $R_1 \rightarrow T_1$ whose weights are similar in either case. When T_2/R_2 increases, the contribution of R_2–T_2 shows a large difference in the two types of signal.

The lines through the data in Figure 6 are simulations using eq 2 for fluorescence and eq 3 for the ligand isosbestic signal, with the values for L and c determined from simulations of 436-nm absorbance data. The two curves at pH 7 are similar and indicate little contribution from the doubly liganded states. The data at lower pH indicate the formation of more T_2 (larger L value). These data are consistent with the assumption that the signal for the ligand isosbestic absorbance change is proportional to the number of deoxyhemes making the R–T transition. The fraction of the absorbance signal (436 nm) for ligand recombination is by definition the fraction photolyzed (z) and is represented by the straight line of slope 1.

Departure from the Two-State Model. Although a description of the kinetics as well as the amplitudes of the reactions is a complex undertaking, a semiquantitative analysis readily shows a deviation from the two-state model. As already mentioned, the major new finding is the excess amplitude of the rapid phase of ΔF which cannot be accommodated within a model having only two states.

To better visualize the contribution of the 10 substates to the observed signals, consider the diagram in Figure 8. Initially, all tetramers exist as R_4, and the laser pulse creates a distribution of R states, which come to equilibrium with the corresponding T state. Figure 8 represents a snapshot just after the R to T equilibrium is established, but before appreciable ligand recombination. The parameters are approximately those for samples at pH 6.5 and 0.1 atm of CO, where $T_2/R_2 \cong 1$. The arrows represent the relative (log) rates. With three or four ligands bound, the R state is heavily favored, and the T states are never populated; the rates involved are unknown (shown as dashed lines).

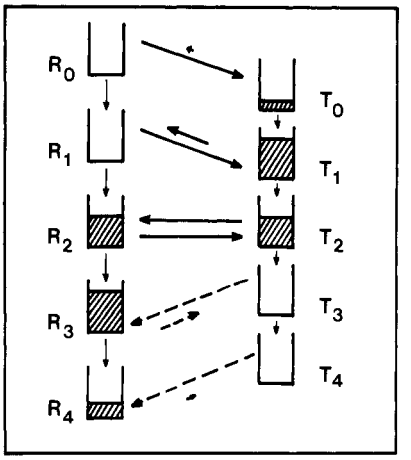

FIGURE 8: Diagram of the 10 substates involved in the allosteric model for Hb tetramer. The populations in each well represent a snapshot at 0.5 ms after a flash of 50% photolysis. For the parameters used (R to T rate of 10^4/s, R-state binding rate of 200/s, $L = 2.5 \times 10^5$, and $1/c = 500$, implying $T_2/R_2 = 1$), this time frame is just after the R to T equilibrium and before appreciable ligand recombination.

As an example, consider tetramers initially in the R_0 state; the dominant pathway to return to the ground state is R_0–T_0–T_1–T_2–R_2–R_3–R_4. The rate-limiting step of this relaxation is the slow ligand binding to the T states. Tetramers initially in the R_3 state simply return rapidly and make little contribution to ΔF. The most interesting case is R_2 tetramers that first come to equilibrium with T_2. The T_2 formed later returns as R_2 is depleted by binding a ligand, forming R_3. The pathway for these tetramers is R_2–T_2–R_2–R_3–R_4, which occurs with the rapid R-state binding rate.

As shown in Figures 4 and 5, the fast phase of ΔF at pH 6 exceeds 40% of the maximum fluorescence signal. Since dye bound originally to states T_0 and T_1 is released at the slow rate, the main contributor to the fast phase in ΔF is conversion of T_2 to R_2. When equilibrium heavily favors R_2, little T_2 is formed and there is no fluorescence signal from these states. For large T_2/R_2, there is a contribution to ΔF, and a fast phase occurs when T_2 drains back through R_2. The normalized amplitude of the fast phase actually observed is even greater than the amount of R_2 formed. Since the fluorescence signal is normalized with respect to the maximum ΔF (i.e., the signal for conversion from R_0 to T_0), the excess fast signal due to conversion of T_2 to R_2 requires a larger weight than for the same number of tetramers converting as R_0–T_0. This implies a higher dye affinity for the T_2 state.

This difference of affinity within the T states implies a dependence of the relative amount of fast ΔF on [HPT], since with large excess of dye each T state will bind one dye molecule and have equal weights. At [HPT] < [Hb] the T states compete for dye, and if T_2 binds dye with a higher affinity than T_0, then the fast ΔF will be enhanced. This effect was, in fact, observed (Figure 5), and the curve for [HPT]/[Hb] = $^1/_4$ at pH 6 can be simulated if the T_2 state is given a weight 4 times that of T_0. The asymmetry about $z = 0.5$ in the curves is also predicted since more competition between T_2 and T_0 occurs at large fractional photolysis.

There is other evidence that the doubly liganded tetramer possesses special properties. Work with asymmetric Hb hybrids indicate two types of the doubly liganded tetramer exist, one R-like and one T-like (Cassoly, 1978). This is also evident in the cooperative free energy values for the doubly liganded forms (Smith & Ackers, 1985).

Although the two-state model provides a good general description of the ligand binding kinetics, the present results show

that the Hb tetramer requires more than two states with respect to HPT binding. If ligand binding and dye binding were two independent processes, then the two-state model could still serve for the ligand reactions. However, the dye binding shifts the R–T equilibrium and therefore is strongly coupled to ligand binding. If the binding of effectors to Hb within the erythrocytes (for example, DPG) behaves similarly, then an extension of the two-state model is needed to represent the behavior of Hb under physiological conditions.

ACKNOWLEDGMENTS

We thank Cindy Kimble for technical assistance.

Registry No. CO, 630-08-0.

REFERENCES

Antonini, E., & Brunori, M. (1971) *Hemoglobin and Myoglobin in Their Reaction with Ligands*, North-Holland, Amsterdam.

Blough, N. V., & Hoffman, B. M. (1984) *Biochemistry 23*, 2875–2882.

Blough, N. V., Zemel, H., & Hoffman, B. M. (1984) *Biochemistry 23*, 2883–2891.

Cassoly, R. (1978) *J. Biol. Chem. 253*, 3602–3606.

Duddell, D. A., Morris, R. J., & Richards, J. T. (1980) *Biochim. Biophys. Acta 621*, 1–8.

Edelstein, S. J., & Edsall, J. T. (1986) *Proc. Natl. Acad. Sci. U.S.A. 83*, 3796–3800.

Gibson, Q. H. (1959) *Biochem. J. 71*, 293–303.

Gibson, Q. H. (1978) *Porphyrins 5*, 153–203.

Hamilton, T. D. S. (1971) *J. Phys. E 4*, 326–328.

Johnson, M. L. (1986) *Biochemistry 25*, 791–797.

Johnson, M. L., Turner, B. W., & Ackers, G. K. (1984) *Proc. Natl. Acad. Sci. U.S.A. 81*, 1093–1097.

MacQuarrie, R., & Gibson, Q. H. (1972) *J. Biol. Chem. 247*, 5686–5694.

Miura, S., & Ho, C. (1984) *Biochemistry 23*, 2492–2499.

Monod, J., Wyman, J., & Changeux, J.-P. (1965) *J. Mol. Biol. 12*, 88–118.

Saffran, W. A., & Gibson, Q. H. (1978) *J. Biol. Chem. 253*, 3171–3179.

Sawicki, C. A., & Gibson, Q. H. (1976) *J. Biol. Chem. 251*, 1533–1542.

Shulman, R. G., Hopfield, J. J., & Ogawa, S. (1975) *Q. Rev. Biophys. 8*, 325–420.

Simolo, K., Stucky, G., Chen, S., Bailey, M., Scholes, C., & McLendon, G. (1985) *J. Am. Chem. Soc. 107*, 2865–2872.

Smith, F. R., & Ackers, G. K. (1985) *Proc. Natl. Acad. Sci. U.S.A. 82*, 5347–5351.

Viggiano, G., & Ho, C. (1979) *Proc. Natl. Acad. Sci. U.S.A. 76*, 3673–3677.

Computer Simulations of Cyclic Enkephalin Analogues†

Moises Hassan and Murray Goodman*

Department of Chemistry, University of California, San Diego, La Jolla, California 92093

Received August 20, 1985; Revised Manuscript Received July 14, 1986

ABSTRACT: Molecular dynamics simulations and energy minimization studies of cyclic enkephalin analogues incorporating retro-inverso modifications have been carried out. The dynamic trajectories are analyzed in terms of the relative mobiiity of the 14-membered rings, conformational transitions among equilibrium states, and hydrogen-bonding patterns. The cyclization of the molecules reduces the motion of the ring structures substantially. Time-correlated conformational transitions resulting in the reorientation of peptide units are observed. Hydrogen bonds form principally C_7 structures. Because of the incorporation of retro-inverso residues, C_6 and C_8 structures are also formed. Starting conformations for energy minimizations were obtained from the molecular dynamics simulations and from a systematic search of the conformational space available to the molecules. Several minimum energy backbone and side-chain conformations were found for each analogue. The effect of retro-inverso residues on hydrogen-bonding patterns and backbone conformations is discussed.

Opioid peptides have been of interest as possible substitutes for alkaloid opiate drugs and for their biological importance as natural analgesics. To understand the physiological response triggered by the binding of these molecules, knowledge of the structure of the receptor and the conformation of the opioid is needed. By specifically modifying peptide opiates and monitoring binding, biological activity, and receptor selectivity, the important pharmacophores of the enkephalins have been elucidated. The importance of residues 1, 3, and 4, Tyr, Gly, and Phe, respectively, for biological activity is now well established (Morley, 1980).

The next stage in these studies is the determination of the conformations responsible for the interaction with the receptor. Much work has been carried out on the basis of the assumption that the conformations obtained from the application of experimental or theoretical techniques are relevant to biological activity, and in many cases the preferred conformation resulting from these studies has been directly related to the "active conformtions". Although this is certainly possible, there is no a priori reason why this should be so. The high flexibility of these linear peptides makes the interpretation of the conformational analysis difficult; experimental results yield

† This work was supported by National Institutes of Health Grant AM 15420-15. M.H. is partially supported by CONICIT, a Venezuelan agency.

0006-2960/86/0425-7596$01.50/0